Proc. Natl. Acad. Sci. USA
Vol. 92, pp. 12300–12303, December 1995
Biochemistry

Distance determination in proteins using designed metal ion binding sites and site-directed spin labeling: Application to the lactose permease of *Escherichia coli*

(electron paramagnetic resonance/transmembrane helices/helix packing)

JOHN VOSS*, WAYNE L. HUBBELL†, AND H. RONALD KABACK*‡

*Howard Hughes Medical Institute, Departments of Physiology and Microbiology and Molecular Genetics and †Jules Stein Eye Institute and Department of Chemistry and Biochemistry, University of California, Los Angeles, CA 90095-1662

Contributed by H. Ronald Kaback, September 11, 1995

ABSTRACT **As shown in the accompanying paper, the magnetic dipolar interaction between site-directed metal–nitroxide pairs can be exploited to measure distances in T4 lysozyme, a protein of known structure. To evaluate this potentially powerful method for general use, particularly with membrane proteins that are difficult to crystallize, both a paramagnetic metal ion binding site and a nitroxide side chain were introduced at selected positions in the lactose permease of *Escherichia coli*, a paradigm for polytopic membrane proteins. Thus, three individual cysteine residues were introduced into putative helix IV of a lactose permease mutant devoid of native cysteine residues containing a high-affinity divalent metal ion binding site in the form of six contiguous histidine residues in the periplasmic loop between helices III and IV. In addition, the construct contained a biotin acceptor domain in the middle cytoplasmic loop to facilitate purification. After purification and spin labeling, electron paramagnetic resonance spectra were obtained with the purified proteins in the absence and presence of Cu(II). The results demonstrate that positions 103, 111, and 121 are 8, 14, and >23 Å from the metal binding site. These data are consistent with an α-helical conformation of transmembrane domain IV of the permease. Application of the technique to determine helix packing in lactose permease is discussed.**

In the preceding paper (1), a technique combining protein engineering and site-directed electron paramagnetic resonance (EPR) is described for measuring distances within proteins. Thus, EPR spectra from nitroxides specifically attached at various positions in the long interdomain helix of T4 lysozyme relative to a designed metal binding site were analyzed in order to compare distances calculated using the theoretical analysis of Leigh (2) with the known structure. Calculated distances exhibit excellent correspondence to the distances estimated from modeling based on the x-ray structure of the protein. In addition to its potential for studying protein dynamics, the approach was conceived to obtain structural information for proteins that are difficult to crystallize, particularly integral membrane proteins. In this paper, we describe an application of the technique to the lactose (lac) permease of *Escherichia coli*.

Lac permease is a hydrophobic, polytopic membrane protein that catalyzes the coupled stoichiometric translocation of β-galactosides and H^+ and is encoded by the *lacY* gene, which has been cloned and sequenced (reviewed in refs. 3 and 4). The permease has been solubilized from the membrane, purified to homogeneity, reconstituted into proteoliposomes, and shown to be solely responsible for β-galactoside transport (reviewed in ref. 5) as a monomer (see ref. 6). A secondary-structure model was proposed (7) in which the permease consists of 12 hydrophobic segments in α-helical conformation that traverse the membrane in zigzag fashion connected by hydrophilic domains (loops) with both the N and C termini on the cytoplasmic face (Fig. 1). Evidence demonstrating that the permease is highly helical in nature and confirming the topological predictions of the 12-helix motif has been obtained from various experimental approaches (reviewed in refs. 9–12).

Site-directed and cysteine-scanning mutagenesis have allowed delineation of amino acid residues in lac permease that are essential for active transport and/or substrate binding (reviewed in ref. 13). However, structural information is required to understand the role of these residues in the transport mechanism, and lac permease has not yielded to crystallization attempts thus far. Therefore, development of alternative methods for obtaining structural information is essential. In this respect, a functional permease molecule has been engineered in which all of the native cysteine residues have been replaced [C-less permease (14)], and single cysteine residues have been placed at more than 350 positions in the molecule. In addition to providing evidence that remarkably few amino acid residues play a mandatory role in the transport mechanism, the cysteine-replacement mutants represent unique molecules that are being used to study permease structure and function (15–20). Recent experiments utilizing mutagenesis and site-directed excimer fluorescence have led to a model describing helix packing in the C-terminal half of the permease (13, 15) and the model has been confirmed and extended through the use of designed metal binding sites (i.e., bis-His residues) between transmembrane helices (21–24) and site-directed chemical cleavage (22).

In this communication, the metal–nitroxide approach is applied to lac permease. Three individual cysteine residues were introduced into putative helix IV of a permease mutant devoid of native cysteine residues containing a metal-ion binding site (six contiguous histidine residues) in the periplasmic loop connecting helices III and IV. After spin labeling, EPR spectra were obtained with the purified proteins in the absence and presence of Cu(II). The results are consistent with this portion of the permease in an α-helical conformation.

MATERIALS AND METHODS

Materials. (1-Oxyl-2,2,5,5-tetramethylpyrroline-3-methyl)-methanethiosulfonate (methanethiosulfonate spin label) was a gift from Kálmán Hideg and is available from Reanal (Budapest). Analytical grade $CuCl_2$ was purchased from Aldrich. Buffers used in binding and spectroscopic measurements were made with 18 MΩ distilled water and treated with Chelex-100 resin (Bio-Rad) to remove all trace divalent cations.

The publication costs of this article were defrayed in part by page charge payment. This article must therefore be hereby marked "*advertisement*" in accordance with 18 U.S.C. §1734 solely to indicate this fact.

Abbreviation: EPR, electron paramagnetic resonance.

‡To whom reprint requests should be addressed.

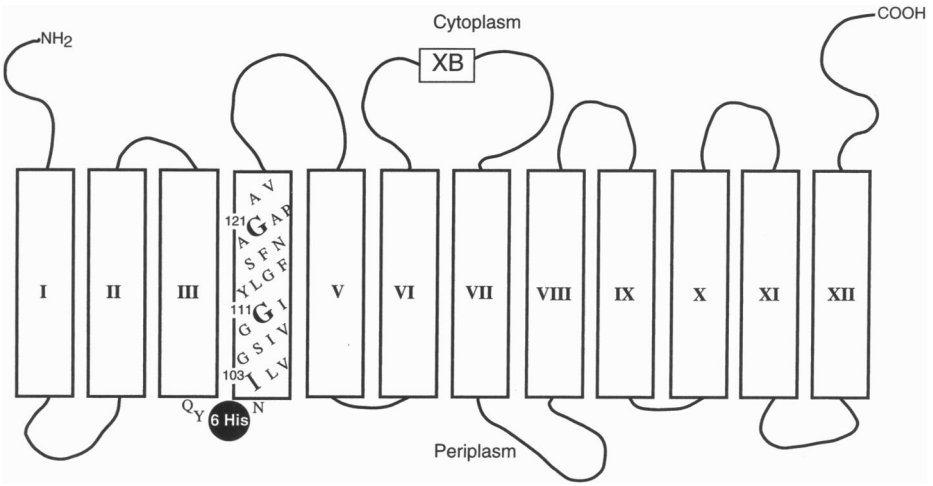

FIG. 1. Secondary structure model of lac permease showing 12 transmembrane α-helices connected by hydrophilic loops with the N and C termini on the cytoplasmic surface of the membrane. The amino acid sequence of helix IV is shown, and the residues that were replaced with cysteine are highlighted. In addition, the position of the 6His insert in the loop between helices III and IV as well as the position of the biotin acceptor domain preceded by a factor Xa protease site (8) in the middle cytoplasmic loop are shown.

Construction, Expression, and Purification of Mutant Lac Permeases. Single cysteine mutants are identified by specifying the original residue, the number of the residue, and the new residue, in that order. As in the preceding paper (1), the spin-labeled side chain is denoted as R1. Mutants with more than one substitution are identified by specifying each mutation separated by a slash.

For construction of mutants (Fig. 1), six contiguous histidine residues were inserted initially into the loop between helices III and IV by using the *lacY* cassette gene (GenBank data base accession no. X56095) encoding C-less permease (14) as described for wild-type permease (25). Individual cysteine replacements for Ile-103, Gly-111, or Gly-121 were then constructed by site-directed mutagenesis using synthetic mutagenic primers and two-step PCR as described (8). Finally, the biotin acceptor domain from a *Klebsiella pneumoniae* oxaloacetate decarboxylase (26) was inserted into the middle cytoplasmic loop of the mutants (27). After confirming the desired mutations by dideoxynucleotide sequence analysis (28, 29), *E. coli* T184 (*lacZ*$^-$*Y*$^-$) was transformed with plasmid encoding a given mutant, grown in 12 L (24 L for mutant 6His/G121C) of LB broth at 37°C, and induced with isopropyl β,D-thiogalactopyranoside. A membrane fraction was prepared and extracted with 3% *n*-dodecyl β,D-maltoside (DM), and the permease was purified by affinity chromatography on immobilized monomeric avidin as described (26).

Transport Measurements. Transport assays were carried out with freshly grown cells transformed with a plasmid encoding a given permease mutant as described (8). [1-^{14}C]Lactose (10 mCi/mmol; 1 Ci = 37 GBq) was used at a final concentration of 0.4 mM, and the measurements were carried out at room temperature.

EPR Spectroscopy. EPR measurements on given spin-labeled lac permease mutants were performed in a quartz capillary at 22°C. Sample (5–10 μl) containing purified permease at a final concentration of ≈20 μM in 10 mM Mes, pH 7.5/0.02% DM was used in each measurement. Spectra were signal averaged over 12 scans with a Varian model E-104 X-band spectrometer fitted with a loop-gap resonator (30) at a microwave power of 2 mW and a modulation amplitude of 2 G.

Data Analysis. Quantitative aspects of the analysis described by Leigh (2) are presented in the accompanying paper (1).

RESULTS

Transport Activity of Mutants. As shown by [1-^{14}C]lactose transport assays in *E. coli* T184 (*lacZ*$^-$*Y*$^-$) (Fig. 2), mutants 6His/I103C and 6His/G111C exhibit initial rates of transport and steady-state levels of accumulation that are comparable to C-less permease. In contrast, although mutant 6His/G121C retains significant activity, it accumulates the disaccharide to a steady state that is only ≈20% of C-less permease in 40 min. As shown by Jung *et al.* (8), G121C permease without the 6His insert exhibits ≈50% of the steady-state level of accumulation of C-less permease and is expressed at a comparable level. Although not shown, Western blot analysis reveals that 6His/I103C and 6His/G111C permeases are expressed at normal levels, while expression of 6His/G121C is markedly reduced, which may account for its low activity.

Metal–Spin Label Interactions in Lac Permease Mutants. To test the feasibility of the metal–nitroxide approach with respect to distance measurements in lac permease, three cysteine residues were introduced individually into helix IV in place of Ile-103, Gly-111, or Gly-121 in C-less permease containing six contiguous histidine residues in the periplasmic loop between helices III and IV (Fig. 1). In addition, each construct contained a biotin acceptor domain in the middle cytoplasmic loop to facilitate purification by avidin affinity chromatography (27). Each mutant was purified, spin labeled,

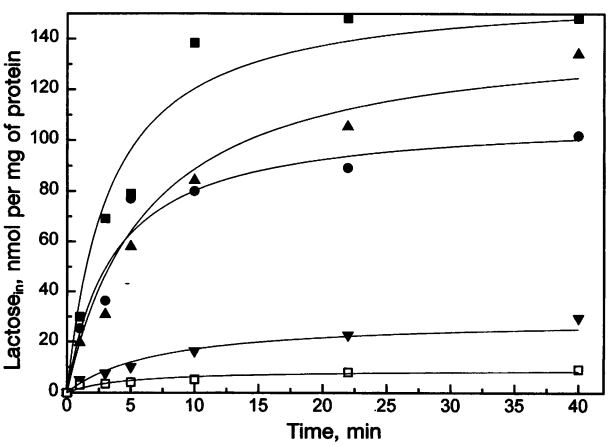

FIG. 2. Transport activity of lac permease constructs. Time courses of [1-^{14}C]lactose transport (nmol·mg^{-1} of total protein) were assayed in *E. coli* T184 (*lacZ*$^-$*Y*$^-$) expressing C-less control (■), 6His/I103C (●), 6His/G111C (▲), or 6His/G121C (▼) permease as described. □, *E. coli* T184 transformed with plasmid devoid of a *lacY* insert.

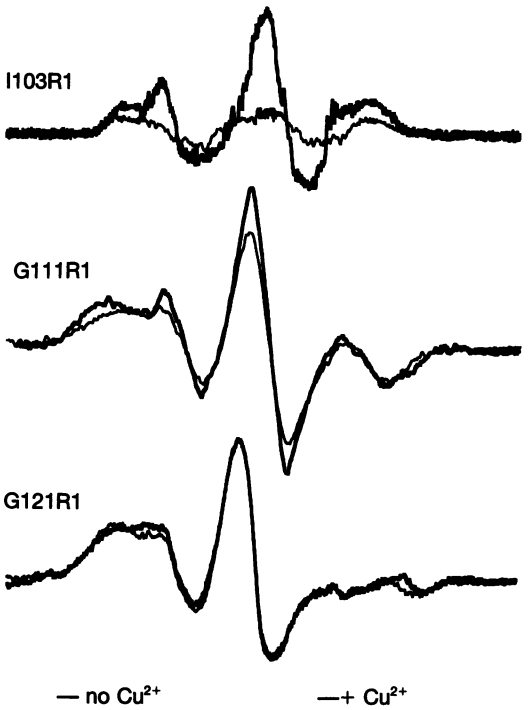

FIG. 3. Effect of Cu(II) on EPR spectra of lac permease spin-labeled at position 103, 111, or 121 (see Figs. 1 and 5). Measurements were made with mutant 6His/I103R1, 6His/G111R1, or 6His/G121R1 in the absence or presence of Cu(II) as described.

concentrated to ≈20 μM, and studied by EPR in the presence or absence of 100 μM Cu(II) (Fig. 3).

Clearly, as observed with the interdomain helix of T4 lysozyme (1), the closer the nitroxide labeled side chain to the metal binding site in the protein sequence, the greater the spectral broadening and decrease in amplitude in the presence of Cu(II). Thus, mutant I103R1 exhibits the most dramatic effect, G111R1 is intermediate, and G121R1 is affected minimally by the presence of Cu(II). The Cu(II) binding site is apparently saturated since increasing the [Cu(II)] to 500 μM does not cause a further decrease in the center line ($m_I = 0$) amplitude (data not shown). The spectra in Fig. 3 reveal that addition of Cu(II) has obvious effects on the lineshapes as well as amplitude, suggesting that metal binding changes local protein conformation. To evaluate the relative contributions of magnetic interactions and conformational changes to the spectral changes, the effect of 500 μM diamagnetic Zn(II) was investigated. The results (not shown) indicate that metal ion binding to the 6His site produces lineshape changes in the hyperfine extrema but no changes in the central ($m_I = 0$) resonance. Thus, intensity changes in this resonance can be attributed to magnetic dipolar interaction.

Table 1. Spectral parameters and calculated distances from the 6His metal binding site of lac permease for nitroxides at residues 103, 111, and 121

Mutant	I/I_0	δH_0	$C/\delta H_0$	r_{calc}, Å
I103R1	0.19	5.8	6.9–5.5	8.3–8.6
G111R1	0.740	5.90	0.330–0.250	13.7–14.4
G121R1	0.98	6.1	0.022–0.016	23–24

Amplitudes represent the center line above-baseline magnitudes normalized to the metal-free control. Ratio of the broadened to unbroadened amplitude (I/I_0) and the unbroadened natural linewidth (δH_0) were obtained from the center $m_I = 0$ line from the spectra in Fig. 4. The dipolar interaction coefficient normalized to the natural linewidth, $C\delta H_0$, was obtained from figure 3 in ref. 1 for the given I/I_0. r_{calc}, Calculated interspin distance determined from $r = [(g\beta\mu^2\tau)/(\hbar C)]^{1/6}$, where the range reflects a $C/\delta H_0$ value obtained from a curve for either the rigid lattice or the isotropic case (1).

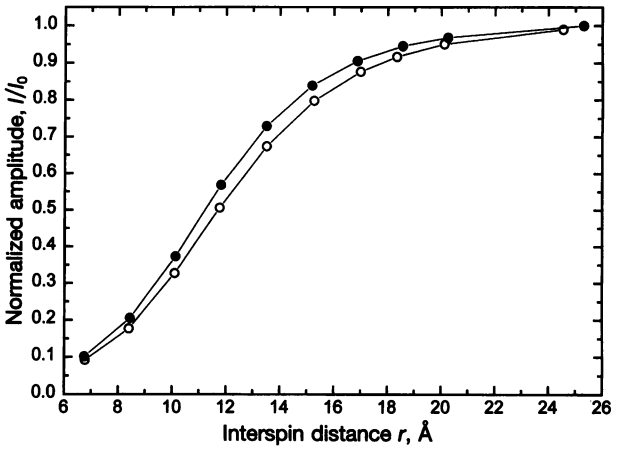

FIG. 4. Plot of the center $m_I = 0$ EPR line amplitude, I, normalized to the metal-free control amplitude, I_0, vs. the interspin distance, r, derived from simulated dipolar-broadened spectra representing either rigid lattice (●) or isotropic rapid motion (○) conditions (see ref. 1). Plot was generated as described (1), although here r is plotted directly on the abscissa using 6 G (average natural linewidth of the spectra examined here) for δH_0.

As discussed in the previous paper (1), estimation of distance between a metal binding site and a nitroxide free radical may be obtained from C, the dipolar interaction coefficient, for the measured spectrum. C is obtained from a plot of the amplitude ratio (I/I_0) vs. the dipolar broadening coefficient normalized to the natural linewidth ($C/\delta H_0$), the values of which arise from spectra broadened by computer simulation (1, 2). Since the spectra analyzed here are neither isotropic nor completely anisotropic, values of C were taken from plots of I/I_0 vs. $C/\delta H_0$ for both isotropic and rigid lattice $m_I = 0$ line amplitudes. The amplitude ratio (I/I_0) for the $m_I = 0$ line of the spectra in Fig. 3 is given in Table 1. For simplicity, plots of the amplitude ratio (I/I_0) vs. interspin distance, r, for a δH_0 value corresponding to the average linewidth (5.9 ± 2 G) are shown in Fig. 4. The calculated distances for positions 103, 111, and 121 are approximately 8, 14, and >23 Å, respectively, from the metal binding site (Table 1).

DISCUSSION

A primary objective of developing metal–spin-label interactions as a means to measure distances in proteins is the potential application of the technique to proteins that are difficult to crystallize. EPR measurements with lac permease containing a metal ion binding site in the periplasmic loop between putative helices III and IV and three cysteine residues downstream from the metal binding site in helix IV indicate that positions 103, 111, and 121 are approximately 8, 14, and >23 Å, respectively, from the metal binding site. Since the closest distance falls below the lower limit of Redfield theory using a relaxer with $T_{1e} \approx 3 \times 10^{-9}$ (i.e., <10 Å), this distance should be interpreted qualitatively (1). A molecular model of transmembrane domain IV with the R1 substitutions at the three positions studied, and the copper ion at the approximate center of the 6His insertion, is shown in Fig. 5. The interspin distances of the modeled α-helix are consistent with the distances obtained from analysis of the EPR spectral broadening.

The results indicate that the method described here can be used to determine helix packing by estimating distances between a designed metal site in one region of the permease and site-directed spin labels in the transmembrane helices. In this

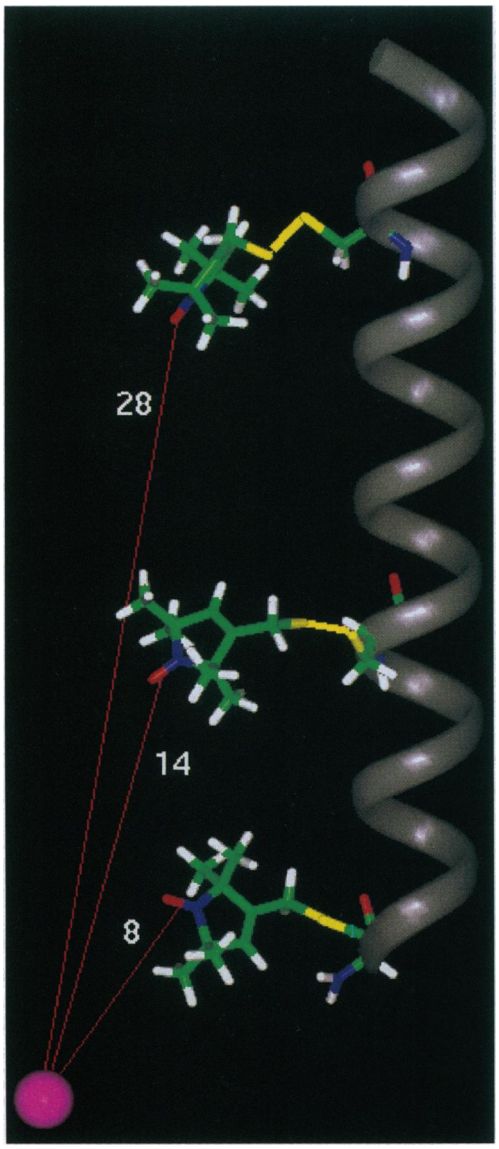

FIG. 5. Model of helix IV in lac permease showing a metal ion in the periplasmic loop between helices III and IV and R1 side chains at residues 103, 111, and 121. All three R1 side chains are shown for illustration, although only one R1 side chain is present in any particular sample. Cu(II)–nitroxide distances (Å) were estimated using INSIGHT II (Biosym Technologies, San Diego) between a conformationally relaxed nitroxide and a Cu atom bound at the approximate center of the 6His metal binding site, which, for clarity, is not shown.

regard, the metal–nitroxide approach has several advantages over other spectroscopic techniques for distance determinations. Room temperature allows detection of time-dependent conformational changes. Furthermore, the method does not suffer from the orientation ambiguity and background problems inherent in fluorescence energy transfer.

It has been demonstrated recently that in addition to the loops (25), metal binding sites in the form of bis-His residues can be engineered into the transmembrane helices of the permease, while the wild-type enzyme does not bind metal (21–24). Since the dimensions of the permease approximate 44 × 50 Å (31, 32), it may be necessary to make the measurements from two metal binding sites inserted independently on the surfaces or within the permease. On the other hand, as discussed in the preceding paper (1), metal–nitroxide interactions have the potential to probe longer distances. By using the bound metal as a reference point, helix packing can be determined by triangulation of distances measured from spin labels attached to single cysteine residues in each transmembrane helix. Moreover, by utilizing three sets of constructs with a metal binding site and a single cysteine residue in each transmembrane domain at approximately the same depth in the permease, it should be possible to obtain overlapping measurements, which will allow an assessment of helix tilting as well. Finally, by utilizing the engineered metal binding sites in conjunction with spin-labeled galactoside analogs (33, 34), it should be possible to localize the substrate binding site(s) in the permease.

We thank Heinrich Jung and Jianhua Wu for helpful discussions. We are also indebted to Kerstin Stempel for synthesizing oligodeoxynucleotides. This work was supported in part by National Institutes of Health Grant EY05216 to W.L.H. and by the Jules Stein Professor endowment.

1. Voss, J., Salwinski, L., Kaback, H. R. & Hubbell, W. L. (1995) *Proc. Natl. Acad. Sci. USA* **92,** 12295–12299.
2. Leigh, J. S. (1970) *J. Chem. Phys.* **52,** 2608–2612.
3. Kaback, H. R. (1976) *J. Cell. Physiol.* **89,** 575–593.
4. Kaback, H. R. (1983) *J. Membr. Biol.* **76,** 95–112.
5. Viitanen, P., Newman, M. J., Foster, D. L., Wilson, T. H. & Kaback, H. R. (1986) *Methods Enzymol.* **125,** 429–452.
6. Sahin-Tóth, M., Lawrence, M. C. & Kaback, H. R. (1994) *Proc. Natl. Acad. Sci. USA* **91,** 5421–5425.
7. Foster, D. L., Boublik, M. & Kaback, H. R. (1983) *J. Biol. Chem.* **258,** 31–34.
8. Jung, K., Jung, H., Colacurcio, P. & Kaback, H. R. (1995) *Biochemistry* **34,** 1030–1039.
9. Kaback, H. R. (1986) *Annu. Rev. Biophys. Biophys. Chem.* **15,** 279–319.
10. Kaback, H. R. (1989) *Harvey Lect.* **83,** 77–103.
11. Kaback, H. R. (1992) *Int. Rev. Cytol.* **137A,** 97–125.
12. Kaback, H. R., Jung, K., Jung, H., Wu, J., Privé, G. G. & Zen, K. (1993) *J. Bioenerg. Biomembr.* **25,** 627–636.
13. Kaback, H. R., Frillingos, S., Jung, H., Jung, K., Privé, G. G., Ujwal, M. L., Weitzman, C., Wu, J. & Zen, K. (1994) *J. Exp. Biol.* **196,** 183–195.
14. van Iwaarden, P. R., Pastore, J. C., Konings, W. N. & Kaback, H. R. (1991) *Biochemistry* **30,** 9595–9600.
15. Jung, K., Jung, H., Wu, J., Privé, G. G. & Kaback, H. R. (1993) *Biochemistry* **32,** 12273–12278.
16. Jung, H., Jung, K. & Kaback, H. R. (1994) *Protein Sci.* **3,** 1052–1057.
17. Jung, K., Jung, H. & Kaback, H. R. (1994) *Biochemistry* **33,** 3980–3985.
18. Wu, J. & Kaback, H. R. (1994) *Biochemistry* **33,** 12166–12171.
19. Wu, J., Frillingos, S., Voss, J. & Kaback, H. R. (1995) *Protein Sci.* **3,** 2294–2301.
20. Wu, J., Frillingos, S. & Kaback, H. R. (1995) *Biochemistry* **34,** 8257–8263.
21. Jung, K., Voss, J., He, M., Hubbell, W. L. & Kaback, H. R. (1995) *Biochemistry* **34,** 6272–6277.
22. He, M. M., Voss, J., Hubbell, W. L. & Kaback, H. R. (1995) *Biochemistry*, in press.
23. He, M. M., Voss, J., Hubbell, W. L. & Kaback, H. R. (1995) *Biochemistry*, in press.
24. Wu, J., Perrin, D., Sigman, D. & Kaback, H. (1995) *Proc. Natl. Acad. Sci. USA* **92,** 9186–9190.
25. McKenna, E., Hardy, D. & Kaback, H. R. (1992) *Proc. Natl. Acad. Sci. USA* **89,** 11954–11958.
26. Cronan, J. E., Jr. (1990) *J. Biol. Chem.* **265,** 10327–10333.
27. Consler, T. G., Persson, B. L., Jung, H., Zen, K. H., Jung, K., Prive, G. G., Verner, G. E. & Kaback, H. R. (1993) *Proc. Natl. Acad. Sci. USA* **90,** 6934–6938.
28. Sanger, F., Nicklen, S. & Coulson, A. R. (1977) *Proc. Natl. Acad. Sci. USA* **74,** 5463–5467.
29. Hattori, M. & Sakaki, Y. (1986) *Anal. Biochem.* **152,** 1291–1297.
30. Froncisz, W. & Hyde, J. S. (1982) *J. Magn. Reson.* **47,** 515–521.
31. Costello, M. J., Escaig, J., Matsushita, K., Viitanen, P. V., Menick, D. R. & Kaback, H. R. K. (1987) *J. Biol. Chem.* **262,** 17072–17082.
32. Li, J. & Tooth, P. (1987) *Biochemistry* **26,** 4816–4823.
33. Gnewuch, T. & Sosnovsky, G. (1986) *Chem. Rev.* **86,** 203–238.
34. Struve, W. G. & McConnell, H. M. (1972) *Biochem. Biophys. Res. Commun.* **49,** 1631–1637.